

# Thermal Transport Calculations for Crystals and nanostructures based on the Boltzmann Transport Equation

---

Jesús Carrete Montaña <[jesus.carrete.montana@tuwien.ac.at](mailto:jesus.carrete.montana@tuwien.ac.at)>

2023-06-14



TECHNISCHE  
UNIVERSITÄT  
WIEN

# A workflow for the thermal conductivity of bulk crystalline solids

# Practical heat management challenges

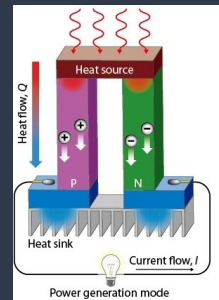
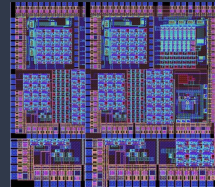
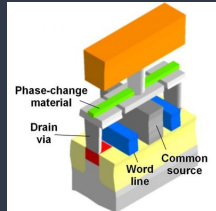
**Power electronics:** Increase heat dissipation per unit area

**Data storage:** Increase thermal efficiency of phase-change memories

**Nanoscale CMOS:** Precise design of heat pathway at the nanometer level

**High-temperature turbines:** Lower alloy temperature by reducing thermal conductivity of coatings

**Thermoelectricity:** Decrease  $\kappa$  to increase  $ZT = \frac{\sigma S^2}{\kappa} T$



$\kappa_\ell$  is the dominant factor in common scenarios

# Lattice-dynamical calculations

## A truncated power-series potential energy model

$$E_{\text{pot}} = E_0 + \frac{1}{2!} \sum_{\substack{a,b \\ \alpha,\beta}} \phi_{ab}^{(\alpha\beta)} x_a^{(\alpha)} x_b^{(\beta)} + \frac{1}{3!} \sum_{\substack{a,b,c \\ \alpha,\beta,\gamma}} \phi_{abc}^{(\alpha\beta\gamma)} x_a^{(\alpha)} x_b^{(\beta)} x_c^{(\gamma)} + \frac{1}{4!} \sum_{\substack{a,b,c,d \\ \alpha,\beta,\gamma,\delta}} \phi_{abcd}^{(\alpha\beta\gamma\delta)} x_a^{(\alpha)} x_b^{(\beta)} x_c^{(\gamma)} x_d^{(\delta)} + \dots$$

Symbols:

- $a, b, c, d \dots$ : atom indices
- $\alpha, \beta, \gamma, \delta \dots$ : Cartesian directions
- $x_a^{(\alpha)}$ : Atomic displacements from the energy minimum
- $\phi_{a_1 a_2 a_3 \dots a_k}^{(\alpha_1 \alpha_2 \alpha_3 \dots \alpha_k)}$ :  $k$ -th order interatomic force constant (IFC)

Most basic incarnation:  $\phi_{a_1 a_2 a_3 \dots a_k}^{(\alpha_1 \alpha_2 \alpha_3 \dots \alpha_k)} = \frac{\partial^k E_{\text{pot}}}{\partial x_{a_1}^{(\alpha_1)} \partial x_{a_2}^{(\alpha_2)} \partial x_{a_3}^{(\alpha_3)} \dots \partial x_{a_k}^{(\alpha_k)}}$

# The lattice thermal conductivity in ordered, weakly anharmonic semiconductors

- Two ingredients:

- Phonon band structure (from  $\phi_{ab}^{\alpha\beta}$ )
- Phonon scattering (from  $\phi_{abc}^{\alpha\beta\gamma}$ )

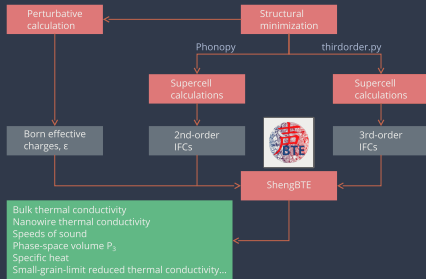
$$\kappa_{\omega}^{\alpha\beta} = \frac{1}{k_B T^2 V N} \sum_{\lambda} f_0 (f_0 + 1) (\hbar\omega_{\lambda})^2 v_{\lambda}^{\alpha} F_{\lambda}^{\beta}$$

- Scattering  $\simeq$  anharmonic + isotopic
- $F_{\lambda}$  satisfies the linearized Boltzmann transport equation for phonons

$$F_{\lambda} = \tau_{\lambda}^0 (v_{\lambda} + \Delta_{\lambda})$$

- Coefficients determined by
  - Allowed 3ph processes
  - Third-order IFCs

Example workflow:

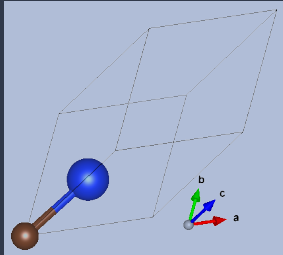


> 99% of time spent on the third-order part

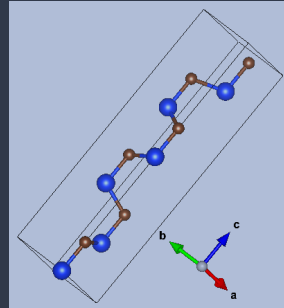
Details: Wu Li, J. Carrete, N. A. Katcho, N. Mingo, Computer Physics Communications 185 (2014) 1747–1758

# How many DFT calculations are required?

SiC, 3C phase



SiC, 6H phase



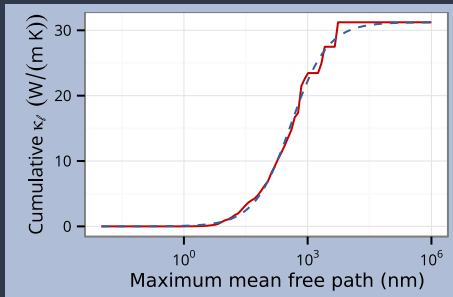
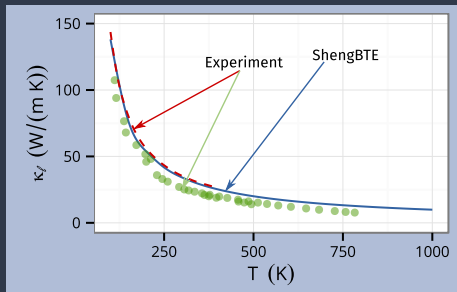
- 216 DFT runs

- 56754 third-order IFCs

- 1644 DFT runs

- 355752 third-order IFCs

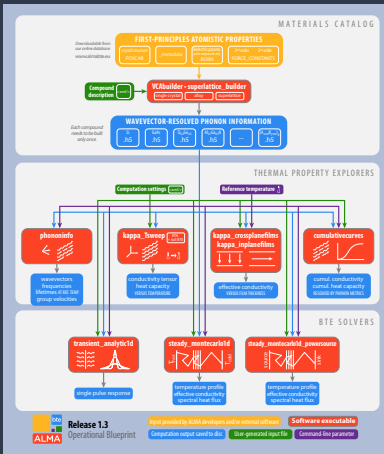
## Comparison with experiment: InAs



- Typically within 5% – 10%
- Very detailed results
- Predictive for not-yet-measured systems

[W. Li, J. Carrete, N. A. Katcho & N. Mingo, Comput. Phys. Commun. 185 (2014) 1747]

# Beyond this model



[J. Carrete et al.,  
Comput. Phys. Commun. 220 (2017) 351]

## Scattering and Green's functions

Bounded defect (vacancy, substitution, interstitial, antisite...)

⇒ broken translation symmetry

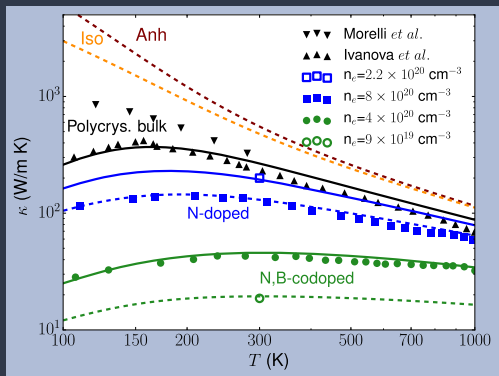
⇒ elastic phonon scattering rates:

$$\Gamma_{\lambda\lambda'} = \frac{\pi}{\omega_\lambda} \left| \left\langle \phi'_\lambda | t^+ | \phi_\lambda \right\rangle \right|^2 \delta(\omega_{\lambda'}^2 - \omega_\lambda^2)$$

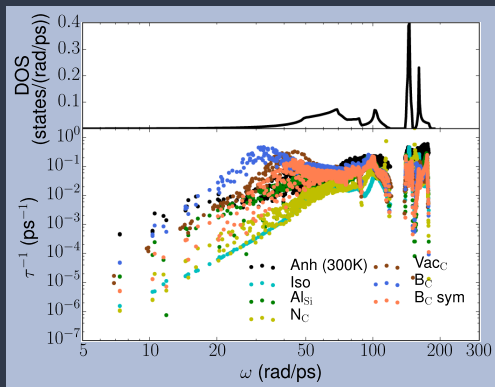
- T matrix:  $t^+ = V(1 - g^+ V)^{-1}$
- Perturbation matrix:  $V := \phi_{2,\text{system}} - \phi_{2,\text{reference}}$
- Causal Green's function:  $g^+(\omega) := \lim_{\eta \rightarrow 0^+} [(\omega^2 + i\eta)1 - K]^{-1}$
- Fermi's golden rule recovered only when  $|g^+ V| \ll 1$
- $V$  requires big supercells, careful relaxation, different charge states...

# Substitutions in 3C-SiC

Comparison with experiments:

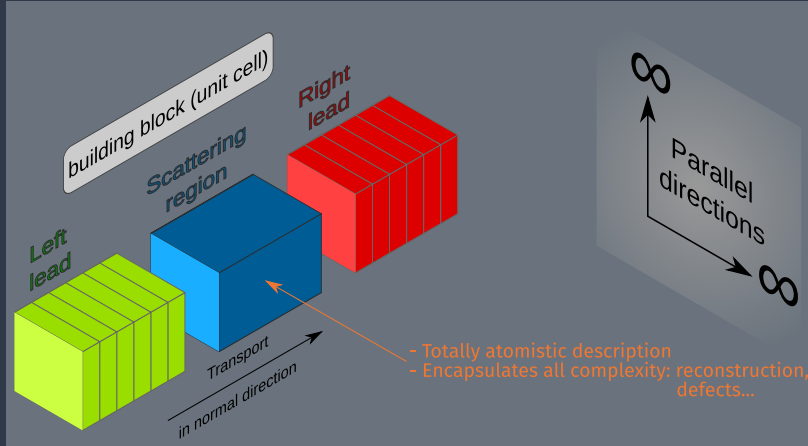


Boron as a superscatterer:



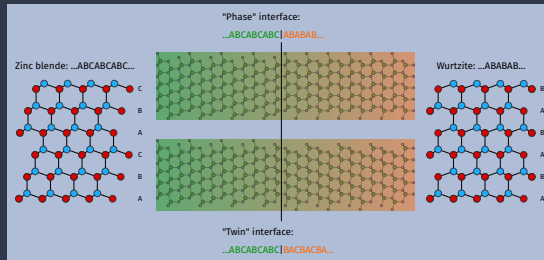
[A. Katre, J. Carrete, B. Dongre, G. K. H. Madsen & N. Mingo, Phys. Rev. Lett. 119 (2017) 075902]

# Transmission at interfaces

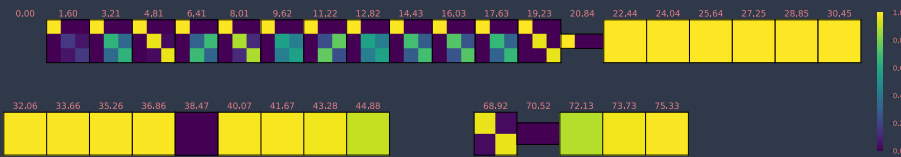


- Requires harmonic IFCs for building blocks of leads + scattering region
- Full details of stable implementation:  
Z.-Y. Ong, J. Appl. Phys., 124 (2018) 151101

# “Phase” and “twin” interfaces in GaP

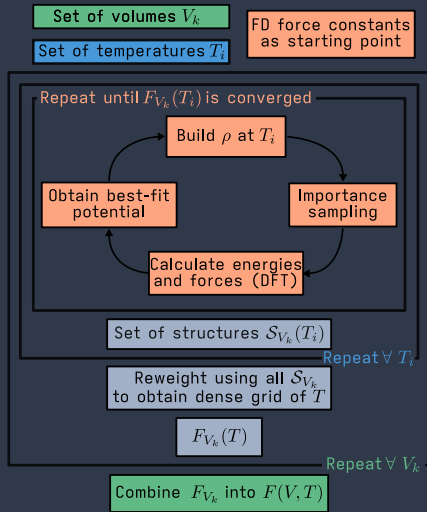


Mode-to-mode transmission as a function of  $\omega$  (rad ps $^{-1}$ )



[J. Carrete, M. López-Suárez, M. Raya-Moreno, A. S. Bochkarev, M. Royo, G. K. H. Madsen, X. Cartoixà, N. Mingo & R. Rurali *et al.*, *Nanoscale* 11 (2019) 16007–16016]

# Effective harmonic potentials



Try to combine:

- Simplicity of harmonic models
- Flexibility of arbitrary IFCs

Common uses:

- Vibrations in finite- $T$  phases [e.g.: cubic perovskites, Phys. Rev. Materials 4 (2020) 113804]
- Strongly  $T$ -dependent vibrational frequencies
- Thermodynamic phase stability

Different approaches, like:

- Perturbation theory + fourth-order IFCs
- Minimization of free-energy functional
- Self-consistency between real-space distribution function and forces

# Higher-order anharmonicity

PHYSICAL REVIEW LETTERS 126, 115901 (2021)

## Ultrahigh Thermal Conductivity of $\theta$ -Phase Tantalum Nitride

Ashis Kundu,<sup>1,2</sup> Xiaolong Yang,<sup>1,2</sup> Jinlong Ma,<sup>1,4</sup> Tianli Feng,<sup>1,5,6</sup> Jesús Carrete,<sup>3</sup> Xulin Ruan,<sup>7</sup> Georg K. H. Madsen,<sup>3</sup> and Wu Li<sup>1\*</sup>

Extracting long-lasting performance from electronic devices and improving their reliability through effective heat management requires good thermal conductors. Taking both three- and four-phonon scattering as well as electron-phonon and isotope scattering into account, we predict that semimetallic  $\theta$ -phase tantalum nitride ( $\theta$ -TaN) has an ultrahigh thermal conductivity ( $\kappa$ ), of 995 and 820  $\text{W m}^{-1} \text{K}^{-1}$  at room temperature along the  $a$  and  $c$  axes, respectively. Phonons are found to be the main heat carriers, and the high  $\kappa$  hinges on a particular combination of factors: weak electron-phonon scattering, low isotopic mass disorder, and a large frequency gap between acoustic and optical phonon modes that, together with acoustic bunching, impedes three-phonon processes. On the other hand, four-phonon scattering is found to be significant. This study provides new insight into heat conduction in semimetallic solids and extends the search for high- $\kappa$  materials into the realms of semimetals and noncubic crystal structures.

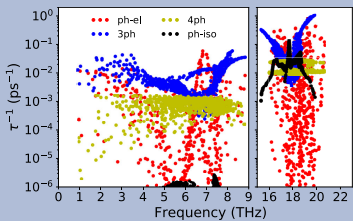


FIG. 3. Calculated three-phonon (3ph), four-phonon (4ph), phonon-isotope (ph-iso), and phonon-electron (ph-el) scattering rates for TaN at 300 K.

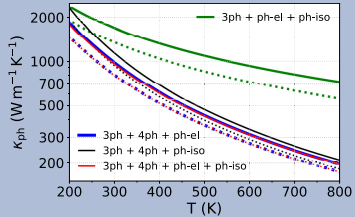


FIG. 4. Temperature dependence of  $\kappa_{\text{ph}}$  in TaN when only certain combinations of phonon scattering mechanisms are considered. The solid and dotted lines correspond to the  $\kappa_{\text{ph}}$  along the  $a$  and  $c$  axes, respectively.

# The machine-learning revolution

# Compressed sensing and IFCs

$$\underbrace{f_a^{(\alpha)}}_{\text{outputs}} = - \sum_b \phi_{ab}^{(\alpha\beta)} \underbrace{x_b^{(\beta)}}_{\text{inputs}} - \frac{1}{2!} \sum_{b,c} \phi_{abc}^{(\alpha\beta\gamma)} \underbrace{x_b^{(\beta)} x_c^{(\gamma)}}_{\text{inputs}} - \frac{1}{3!} \sum_{b,c,d} \phi_{bcd}^{(\alpha\beta\gamma\delta)} \underbrace{x_b^{(\beta)} x_c^{(\gamma)} x_d^{(\delta)}}_{\text{inputs}} + \dots$$

Accelerated workflow:

1. Randomly sample displacement space
2. Use all forces obtained from DFT for each configuration
3. Solve the underdetermined linear regression problems while promoting sparsity

Early work: F. Zhou et al., Phys. Rev. Lett. 113 (2014) 185501

Open-source implementation

[P. Erhart's group]:

<https://hiphive.materialsmodeling.org>



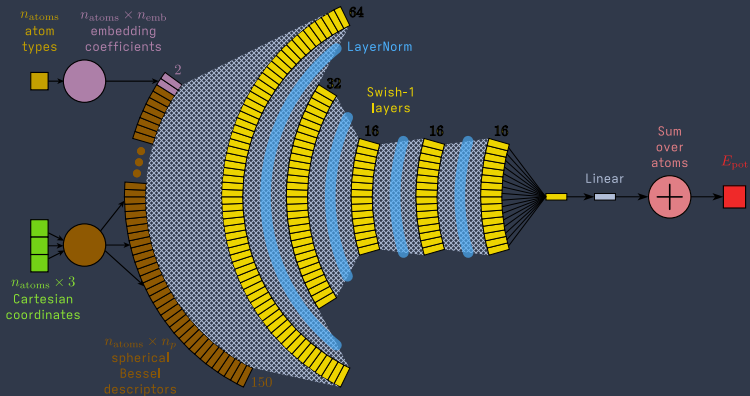
# A neural-network force field

## A Differentiable Neural-Network Force Field for Ionic Liquids

Hadrián Montes-Campos, Jesús Carrete, Sebastian Bichelmaier, Luis M. Varela,  
and Georg K. H. Madsen



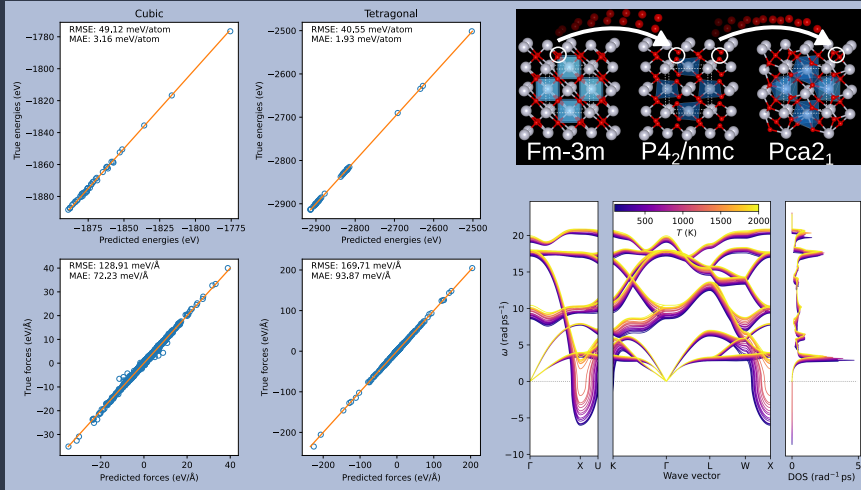
Cite This: *J. Chem. Inf. Model.* 2022, 62, 88–101



Behler-Parrinello model  
with some unique  
features

- End-to-end differentiability
- Orthogonal spherical Bessel descriptors
- 1-cycle learning rate schedule
- Modern activation function
- Normalization to avoid vanishing gradients

# An example application to solids: $\text{HfO}_2$



[S. Bichelmaier, J. Carrete, R. Wanzenböck, F. Buchner & G. K. H. Madsen,  
Phys. Rev. B 107 (2023) 184111]

# Automatic differentiation

NeuralIL is implemented on top



of  
Features:

- Automatic differentiation
- Just-in-time compiler (fast code)
- Vectorization on CPUs, GPUs and TPUs

Foundation of new Google ML ecosystem: Flax, Optax...

AD implements two differential operators using the chain rule systematically:

$$f : \mathbb{R}^n \longrightarrow \mathbb{R}^m$$

- Jacobian-vector product (forward mode):  
 $JVP(f, x \in \mathbb{R}^n, u \in \mathbb{R}^n) \in \mathbb{R}^m$
- Vector-Jacobian product (reverse mode):  
 $VJP(f, x \in \mathbb{R}^n, v \in \mathbb{R}^m) \in \mathbb{R}^n$

Accurate like the function itself, almost as fast, easy and natural to use

# Force constants from automatic differentiation

## Lennard-Jones toy model

```
#!/usr/bin/env python

import numpy.random as random
import jax
import jax.numpy as np

def lj_potential(positions):
    "Lennard-Jones potential in reduced units."
    # Compute all relative positions between pairs without iterating.
    delta = positions[:, np.newaxis, :] - positions
    # Take only the combinations of two different atoms.
    indices = np.triu_indices(positions.shape[0], k=1)
    delta = delta[indices[0], indices[1], :]
    # Compute the squared distances and evaluate the potential energy.
    r2 = (delta * delta).sum(axis=1)
    rm2 = 1. / r2
    rm6 = rm2 * rm2 * rm2
    rm12 = rm6 * rm6
    return (rm12 - 2. * rm6).sum()

lj_gradient = jax.jit(jax.grad(lj_potential)) # Automatic gradient function
lj_hessian = jax.jit(jax.hessian(lj_potential)) # Automatic Hessian function
lj_potential = jax.jit(lj_potential) # Compiled potential function
test_positions = 5. * random.random_sample((20, 3)) # Put 20 particles in a cube of side 5.
e_pot = lj_potential(test_positions)
forces = -lj_gradient(test_positions)
hessian = lj_hessian(test_positions)
```

Same procedure regardless of complexity:

- Forces:  $\text{gradient} = \text{single-shot VJP}$  (row of Jacobian)
- Harmonic IFCs: column-by-column Jacobian of gradient (forward mode composed over reverse mode)
- ...

## Better than force constants: higher-order differential operators

### A truncated power series through nested JVPs

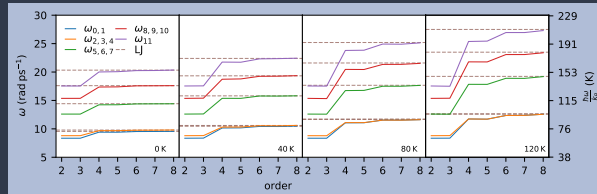
$$E_{\text{pot}} = E_0 + \frac{1}{2!} \sum_{\substack{a,b \\ \alpha,\beta}} \phi_{ab}^{(\alpha\beta)} x_a^{(\alpha)} x_b^{(\beta)} + \frac{1}{3!} \sum_{\substack{a,b,c \\ \alpha,\beta,\gamma}} \phi_{abc}^{(\alpha\beta\gamma)} x_a^{(\alpha)} x_b^{(\beta)} x_c^{(\gamma)} + \frac{1}{4!} \sum_{\substack{a,b,c,d \\ \alpha,\beta,\gamma,\delta}} \phi_{abcd}^{(\alpha\beta\gamma\delta)} x_a^{(\alpha)} x_b^{(\beta)} x_c^{(\gamma)} x_d^{(\delta)} + \dots$$

$$E_{\text{pot}} = \sum_{n=0}^{n_{\max}} \mathcal{T}_n(\mathbf{r}_0, \mathbf{x}), \text{ where } \mathcal{T}_0(\mathbf{r}, t) = E_{\text{pot}}(\mathbf{r}) \text{ and } \mathcal{T}_n(\mathbf{r}, t) = \frac{1}{n} \frac{\partial \mathcal{T}_{n-1}(\mathbf{r}, t)}{\partial \mathbf{r}} \cdot \mathbf{t}$$

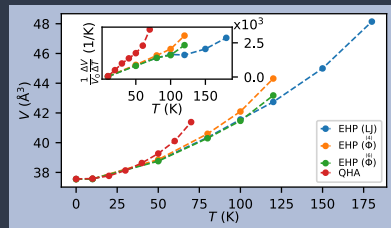
- Trivial to implement
- Avoids catastrophic scaling of number of constants with order

# Example: power-series surrogate models for the LJ clusters and solid

## Effective vibrational frequencies of LJ-6 cluster



Thermal expansion of the LJ crystal:



# The dynamical matrix

## Normal modes in reciprocal space

$$D(q)w_\lambda = \omega_\lambda^2 w_\lambda, \text{ with } D_{a,b}^{(\alpha\beta)}(q) = \frac{1}{\sqrt{m_a m_b}} \sum_{B,B,b} \phi_{0,a}^{(\alpha\beta)} e^{-iq \cdot R_B}$$

Each element of  $D$  is a vector-Hessian-vector product between:

- $\ell(a, \alpha)$ :  $\frac{1}{\sqrt{m_a}}$  for atom  $a$  and direction  $\alpha$  in first unit cell, 0 everywhere else
- $r(q, b, \beta)$ :  $\frac{1}{\sqrt{m_b}} \exp(-iq \cdot R_B)$  for atom  $b$  and direction  $\beta$  in each unit cell  $B$ , 0 everywhere else

## Implementation: JVP of JVP

```
def uHv_complex(p, t, c, u, v):
    """Compute a vector-Hessian-vector product.

    Assume real u and complex v.
    """
    function = lambda x: energy_calculator(x, t, c)
    b_function = lambda x: jax.jvp(function, (x, ), (u, ))[1]
    re_braket = jax.jvp(b_function, (p, ), (v.real, ))[1]
    im_braket = jax.jvp(b_function, (p, ), (v.imag, ))[1]
    return re_braket + 1.j * im_braket
```

- Automatic and efficient
- Similar to DFPT
- Can be done irrep by irrep

## Even more derivatives!

---

A differentiable  $D(q)$  provides automatic access to information within and beyond the harmonic approximation:

- Group velocities:

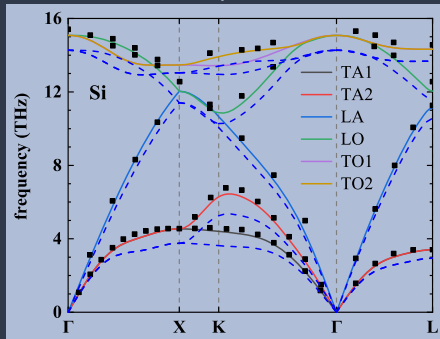
$$v_{g,\lambda}^{(\alpha)} = \frac{\partial \omega_\lambda}{\partial q^{(\alpha)}} = \frac{1}{2\omega_\lambda} \mathbf{w}_\lambda^* \cdot \frac{\partial D(q)}{\partial q^{(\alpha)}} \mathbf{w}_\lambda$$

- Grüneisen parameters:

$$\gamma_\lambda = -\frac{V}{\omega_\lambda} \frac{\partial \omega_\lambda}{\partial V} = -\frac{V}{2\omega_\lambda^2} \mathbf{w}_\lambda^* \cdot \frac{\partial D(q)}{\partial V} \mathbf{w}_\lambda$$

# The transferability of IFCs

Extreme example:



- Solid lines: computed Si spectrum
- Dashed lines: Si spectrum computed with Ge IFCs

Source: G. Guo, X. Yang, J. Carrete and Wu Li,  
J. Phys.: Condens. Matter 33 (2021) 285702

Regression models can detect regularities in diverse families like the half Heuslers

[J. Carrete, Wu Li, N. Mingo, S. Wang & S. Curtarolo, *Phys. Rev. X* 4 (2014) 011019]

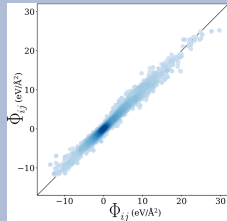
# Regularities within polymorphs of KZnF<sub>3</sub>



J. Chem. Inf. Model. 2018, 58, 2460–2466

## Vibrational Properties of Metastable Polymorph Structures by Machine Learning

Fleur Legrain, Ambroise van Roekeghem, Stefano Curtarolo, Jesús Carrete, Georg K. H. Madsen, and Natalio Mingo



	Pearson coefficient	Spearman coefficient	mean absolute error	root-mean-square error
$\text{tr}(\Phi_0)$	0.99	0.98	0.25 (eV/Å <sup>2</sup> )	0.38 (eV/Å <sup>2</sup> )
$\text{tr}(\Phi_0^2)$	0.98	0.95	0.27 (eV/Å <sup>2</sup> )	0.41 (eV/Å <sup>2</sup> )
$\sqrt{\text{tr}(\Phi_0^2)}$	0.98	0.95	0.28 (eV/Å <sup>2</sup> )	0.43 (eV/Å <sup>2</sup> )
$\Phi_0$ variance	0.99	0.93	0.17 (eV/Å <sup>2</sup> )	0.32 (eV/Å <sup>2</sup> )
$\sqrt{(\bar{w} - \bar{w})^2}$	0.88	0.87	0.88 (rad/ps)	1.14 (rad/ps)
mean $\bar{w}$	0.92	0.88	0.73 (rad/ps)	0.94 (rad/ps)
max $w_{\text{max}}$	0.88	0.87	3.79 (rad/ps)	4.63 (rad/ps)
$C_v$	0.91	0.83	0.0008 (meV/K/atom)	0.0010 (meV/K/atom)
$F_{\text{rb}}$	0.82	0.80	2.92 (meV/atom)	3.78 (meV/atom)
$S_{\text{rb}}$	0.80	0.79	0.009 (meV/K/atom)	0.012 (meV/K/atom)

## Regression model:

- Random-forest regression
- Equivariant inputs (Hessians of scalar descriptors)

## Test system: KZnF<sub>3</sub>

- Cubic perovskite at 0 K
- 121 non-equivalent mechanically stable minima found with USPEX

More specialized than a force field,  
but much cheaper

# Beyond the BTE

## The Allen-Feldman model

The BTE framework is only valid for propagating plane-wave-like modes. On shaky ground when (Ioffe-Regel crossover):

- $\Lambda \sim \pi / |q|$
- $\tau \sim \pi / \omega$

P. B. Allen and J. L. Feldman,  
*Phys. Rev. B* 48 (1993) 12581:

- Vibrational modes (vibrons):  
**Propagons**: phonon-like  
**Diffusons**: delocalized, non-propagating  
**Locons**: localized, non-propagating
- Phonons and diffusons contribute to thermal transport

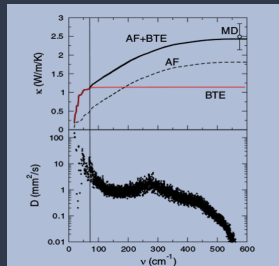
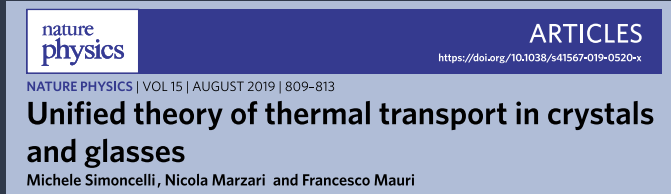


FIG. 4 (color online). Diffusivity of the vibrational modes of a core-shell SiNW with 3 nm diameter and *a*-Si thickness of 1 nm,

Source: D. Donadio, G. Galli,

*Phys. Rev. Lett.* 102 (2009) 195901

# New contributions to the thermal conductivity



Additional non-diagonal term in the thermal conductivity:

$$\kappa^{\alpha\beta} = \kappa_p^{\alpha\beta} + \frac{\hbar^2}{k_B T^2} \frac{1}{VN_c} \sum_{\mathbf{q}} \sum_{s \neq s'} \frac{\omega(\mathbf{q})_s + \omega(\mathbf{q})_{s'}}{2} V^\alpha(\mathbf{q}_{s,s'}) V^\beta(\mathbf{q}_{s',s}) \times \frac{\omega(\mathbf{q})_s \bar{N}(\mathbf{q})_s (\bar{N}(\mathbf{q})_s + 1) + \omega(\mathbf{q})_{s'} \bar{N}(\mathbf{q})_{s'} (\bar{N}(\mathbf{q})_{s'} + 1)}{4(\omega(\mathbf{q})_s - \omega(\mathbf{q})_{s'})^2 + (\Gamma(\mathbf{q})_s + \Gamma(\mathbf{q})_{s'})^2} \times (\Gamma(\mathbf{q})_s + \Gamma(\mathbf{q})_{s'})$$

Non-diagonal terms of the group velocity:

$$V_{\lambda,\lambda'}^{(\alpha)} = \underbrace{\mathbf{w}_{\lambda'}^* \cdot \frac{\partial \sqrt{D(q)}}{\partial q^{(\alpha)}} \mathbf{w}_\lambda}_{\text{automatic differentiation again!}}$$

Important when:

- Phonon frequencies are close (reference: linewidths)
- Non-diagonal elements significant

## Equilibrium molecular dynamics and Green-Kubo

---

$$\kappa^{(\alpha\beta)} \propto \int_0^\infty \left\langle J^{(\alpha)}(0) J^{(\beta)}(t) \right\rangle dt, \text{ with } J = \frac{1}{V} \int x \dot{e}(x) d^3x$$

Pros:

- Compact and elegant formalism
- Anharmonicity and net ionic displacements included (diffusion, liquids...)

Four kinds of problems, important for ab-initio for NN-based MD:

1. Arbitrary assignment of contributions to the energy to individual atoms
2. Expression of  $J$  compatible with periodic boundary conditions
3. Conceptually clear separation of diffusion from conduction in multicomponent systems
4. Poor convergence and noisy character of direct estimates of the average autocorrelation

## Solutions by Baroni and coworkers

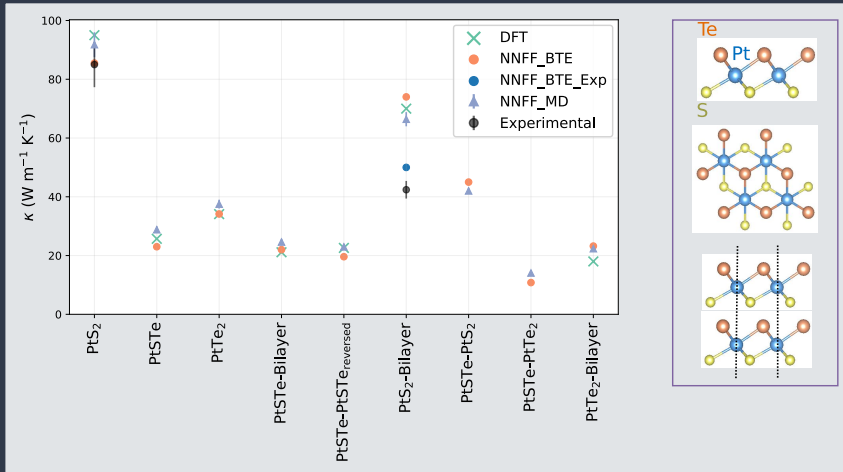
---

1. Gauge invariance vs. choice of atomic contributions to the energy (P. Pegolo, Master Thesis, Università degli Studi di Trieste)
2. Expression of  $J$  based on  $R_n - R_m$  and  $\frac{\partial \epsilon_n}{\partial R_m}$  for an arbitrary potential
3. Spectra of energy and matter fluxes treated together [R. Bertossa *et al.*, Phys. Rev. Lett 122 (2019) 255901]
4. Cepstral analysis of  $J^{(\alpha)}(t)$  to extract low-frequency behavior

Comparison of methods:

P. Pegolo, S. Baroni & F. Grasselli, npj Comput. Mater. 8 (2022) 24

# Comparison of results



[LiJun Pan et al., unpublished]

# Thermal Transport Calculations for Crystals and nanostructures based on the Boltzmann Transport Equation

---

Jesús Carrete Montaña <[jesus.carrete.montana@tuwien.ac.at](mailto:jesus.carrete.montana@tuwien.ac.at)>

2023-06-14



TECHNISCHE  
UNIVERSITÄT  
WIEN